### **FLUORIDE**

### Quarterly Journal of The International Society for Fluoride Research Inc.

## Synaptic Damage in Brain of Mice Exposed to Fluoride and Its Related Occurrence Mechanism

Unique digital address (Digital object identifier [DOI] equivalent): https://www.fluorideresearch.online/epub/files/353.pdf

Qingqing PU<sup>1,2#</sup>, Jie DENG<sup>2,3#</sup>, Ting ZHANG<sup>2,3</sup>, Xiaoxiao ZENG<sup>2,3</sup>, Wenwen HE<sup>2,4</sup>, Yangting DONG<sup>2,3</sup>, Wen WAN<sup>5\*</sup>, Kailin ZHANG<sup>1,2\*</sup>

- <sup>1</sup> Department of Biochemistry and Molecular Biology of Guizhou Medical University, Guiyang, 550004, P. R. China.
- <sup>2</sup> Key Laboratory of Endemic and Ethnic Diseases of the Ministry of Education, Guiyang, 550004, P. R. China.
- <sup>3</sup> Provincial Key Laboratory of Medical Molecular Biology, Guizhou Medical University, Guiyang, 550004, P. R. China.
- <sup>4</sup> Department of Pathology at the First People's Hospital of Guiyang, Guiyang, 550001, P. R. China.
- <sup>5</sup> Department of Forensic Medicine, Guizhou Medical University, Guiyang, 550004, P. R. China.
- # These authors have the equal contribution to the paper.

#### \* Corresponding author:

Kailin Zhang
Department of Biochemistry and
Molecular Biology of Guizhou Medical
University; Key Laboratory of Endemic
and Ethnic Diseases of the Ministry of
Education, Guiyang, 550004, P.R. China.
Tel: +86 13984102293
Email: 476477406@qq.com

Wen Wan
Department of Forensic Medicine,
Guizhou Medical University, Guiyang,
550004, P. R. China.
Tel: +86 15286032152
Email: 811492732@qq.com

Submitted: 2025 May 18 Accepted: 2025 Jun 08 Published as e353: 2025 Jun 08

#### **ABSTRACT**

**Purpose:** The aim of this study is to investigate whether exposure of fluoride induces modification of the synaptic structure and metabolism in brain of mice, as well as to reveal the related molecular mechanisms.

**Methods:** Thirty C57BL/6J mice with one-month-old were used in the experiment. Fluoride (NaF) at the added concentrations of 0 (untreated as normal control), 50 and 100 ppm in drinking water were administered to the mice, respectively, for 3 months. At the end of the experiment, the occurrence of dental fluorosis and fluoride contents in bone and urine, and brain morphology of mice were examined. The synaptic structure of the brain was detected by chemical staining. The protein and mRNA expressions of synaptic activity-regulated cytoskeletal-associated protein (Arc) and N6-methyladenosine (M6A)-related methyltransferase-like 3/14 (METTL3 and METTL14) and fat mass and obesity-associated protein (FTO) were detected by western blotting and real-time PCR, respectively.

**Results:** The results showed that in the mice exposed to fluoride, dental fluorosis and increased fluoride contents in born and urine were found; the abnormal histology and the decreased dendritic spines in the brain detected; the protein expressions (but mRNAs) of Arc and METTL3 were decreased; no significant changes in the protein and mRNA expressions of METTL14 and FTO in brain; interestingly, the decrease in the protein level of Arc or METTL3 was significantly correlated with the increase of fluoride content in urine caused by fluoride exposure.

**Conclusion:** The results indicated that excessive fluoride intake caused damage to the synaptic structure and reduction of Arc protein in the brain of mice, which in mechanism might be involved to the decreased expression of METTL3.

Keywords: Fluoride, Brain, Synapse, Arc, M6A modification, METTL3

### INTRODUCTION

Excessive intake of fluoride can lead to neuropathological changes and neurobehavioral abnormalities in humans and experimental animals. Epidemiological evidence indicates that long-term exposure of the population to a high-fluoride environment can lead to cognitive impairment and mental retardation. Even lower levels of fluoride exposure can affect children's mental development

with a dose-response relationship.<sup>3</sup> It has been indicated that fluoride can be accumulated in brain by crossing the blood-brain barrier, which results in neurotoxicity and impairments in learning and memory.<sup>4</sup> Importantly, fluoride exposure can lead to neurological damage through various complex mechanisms, including the disturbances in synaptic transmission and synaptic plasticity, premature death of neurons, deficits in neurotrophic and transcriptional

factors, disrupted oxidative stress, metabolic changes and inflammatory processes.<sup>5</sup>

Recent studies have shown that fluoride can induce synaptic structural and functional changes, which can impair the ability of learning and memory in animals.6 Synaptic structure injury is one of the important mechanisms of central nervous system injury in chronic fluorosis. Numerous animal experiments have confirmed that fluoride exposure in rats reduces the density of dendritic branches and spines in hippocampal neurons, decreases neuron post-synaptic density (PSD), and widens synaptic gaps, suggesting weakened synaptic connections.7 In addition, fluoride exposure resulted in hyperphosphorylated AMPactivated protein kinase and collapsin responsemediator protein-2 in the hippocampus of rats, which leads to synaptic damage.8 This may be an important cause of memory impairment in fluorosis, offering new insights into the mechanism of fluoride-induced neurotoxicity.

It is worth noting that activity-regulated cytoskeleton-associated protein (Arc), a synapse-specific immediate early gene, is linked to neurological disorders like Alzheimer's Disease (AD), schizophrenia, depression, autism, Angelman syndrome, and fragile X syndrome. The mRNA of Arc can rapidly move to activate the dendrites of the neurons after induction and then is translated into proteins localized at the base of dendritic protrusions, which influences synaptic plasticity by interacting with the neuronal skeleton. In addition, Arc influences actin stability and changes the shape of neuronal dendritic spines by modifying cofilin phosphorylation.

Interestingly, the effects of N6-methyladenosine (m6A) on mRNAs are mediated by a series of progressively discovered m6A readers, writers and erasers. The methyl group can be written on the adenosine base at the nitrogen-6 position of the target mRNA by methyltransferase-like 3/14 (METTL3 and METTL14).12 Recent studies highlight m6A as crucial for synaptic plasticity regulation. As the most common modification in eukaryotic mRNAs and IncRNAs, especially in the brain, m6A influences RNA functionstranscription, splicing, localization, degradation, translation, and transport-by modulating methylationdependent RNA-protein interactions.<sup>13</sup> Recently, it was found that fluoride induced gut microbiota alteration mediates severe intestinal cell injury by inducing m6A modification-mediated ferroptosis.14

Knockdown of YTH nucleic acid binding domain containing 1 (YTHDF1), an RNA-binding protein that plays a crucial regulatory role, in hippocampal neurons causes synaptic dysfunction, including immature spine morphology, impaired excitatory synaptic transmission, reduced PSD-95, and decreased surface expression of alpha-amino-3-hydroxy-5-methyl-4-isoxazolepropionic acid receptor subunit GluA1.<sup>15</sup>

Fluoride exposure increased the m6A level of solute carrier family 7 member 11 (SLC7A11) mRNA, promoted YTHDF2 binding to m6A-modified SLC7A11 mRNA, drove the degradation of SLC7A11 mRNA, and led to a decrease in its protein expression, which eventually triggers ferroptosis. 14 Similarly, METTL14 knockdown in striatal neurons lowers m6A levels in transcripts related to neuron- and synapse-specific proteins.<sup>16</sup> A study indicated that AD mice exhibited increased METTL3 and decreased Fat mass and obesityassociated protein (FTO) in the hippocampus, leading to abnormal mRNA m6A modifications affecting dendritic and synaptic development and glutamate receptor signaling.<sup>17</sup> This disruption in m6A balance may be a key factor in synaptic dysfunction, but its role in synaptic damage by chronic fluorosis remains unexplored.

This study detected the effect of m6A-modified enzymes on synaptic injury in mice with chronic fluorosis. Our research results indicate that METTL3-mediated m6A modification plays a role in fluoride-induced synaptic injury, and Arc may be a potential target.

#### **MATERIALS AND METHODS**

#### Experimental animals

Thirty C57BL/6J mice (clean grade), 15-25 g, were provided by the Animal Experimental Center of Guizhou Medical University in China. They were kept at 22-25°C with 30-55% humidity and acclimatized for one week before treatment.

These mice were divided randomly into the following three groups (5 males and 5 females each), i.e., the untreated control group with tape drinking water (<0.5 ppm fluoride), the small dose fluoride group with drinking water containing 50 ppm fluoride (NaF) and the high-dose fluoride group with 100 ppm fluoride in their drinking water. All mice were fed with standard laboratory chow ad libitum. Mice were housed in stainless steel cages suspended in stainless steel racks and the experiment period was 3 months.

At the end of the study, dental fluorosis was observed and 24-hr urine collected. After collecting urine from mice within 24 hrs and storing it at -80°C, the mice were sacrificed by euthanasia. Parts of brain tissues were preserved in Golgi stain fixing solution. The right of remained hemispheres was kept in 4% paraformaldehyde for morphological observation, while hippocampal tissues from left hemispheres were kept at -80°C for total RNA extraction and protein analysis. The protocol of the animal study was preapproved by the Institutional Animal Care and Ethics Committee of Guizhou Medical University, China (Approval No: 2201322).

### Dental fluorosis observed and fluoride content in urine and bone detected

Dental fluorosis was evaluated referring the Dean's method<sup>18</sup> with white or pigmented bands (I), gray enamel (II) and even loss of tooth structure (III). The fluoride contents in urine and bone were determined by using a CSB-FI fluoride ion electrode (Changsa Analysis Instrumentation, China). In brief, the total ionic strength adjustment buffer I (TISAB I) was prepared. Vertebrae from mice were dry-ashed by utilizing a muffle furnace for 5 hrs at 550°C. The resulting bone ash (20 mg) was mixed with 5 ml of 0.5 M HCl, then combined with TISAB. Urine sample was centrifuged at 1500×g for 5 min and the supernatant mixed with TISAB I. The above final solution was used to measure the fluoride concentration by fluoride ion-selective electrode.

### Histopathological observations of mouse brain

The brain tissues were fixed with 4% paraformaldehyde, embedded in paraffin, and sliced with a thickness of 4  $\mu$ m. After that, the slices were stained with hematoxylin and eosin (HE) for routine pathological examination and with Nissl staining for observing Nissl bodies under a light microscope. The stained slices were scanned with a Digital tissue section scanner (Pannoramic MIDI, 3D Histech, Hungary) and the density of Nissl bodies were blind measured using Image J software.

#### Golgi staining

The fresh brain tissues were rinsed with distilled water to remove blood on the surface and submerged into the Golgi staining fixative in the dark at room temperature (RT) for 14 days. The fixative was changed with the refreshed one after 48 hrs and then every 3 days. Subsequently, these samples were stored in tissue treatment solution at 4°C for 3 days in the dark. Later, brain sections (60  $\mu m$ ) were cut using the vibrating microtome, and gelatinized slides mounted with the tissue treatment solution and dried at RT. Finally, the slices were developed with Golgi developer solution for 30 min and sealed with glycerin gelatin. The stained slices were scanned, and the density of dendritic spine and the number of branches were blind measured using Image J software.

#### Immunohistochemical staining (IHC)

Paraffin-embedded brain sections were dewaxed in xylol solution, and rehydrated and rinsed in PBS. Antigen retrieval was performed by boiling in a citric acid buffer (0.01 mol/l, pH 6.0), followed by incubation with 5% goat serum for one hr at RT. The sections were then incubated with the following primary antibodies: METTL3 (1:200, Abcam, USA), METTL14 (1:800,

Proteintech, USA), FTO (1:500, Proteintech, USA), and Arc (1:200, Abcam, USA) at 4°C overnight. After that, the primary antibody was retrieved, and the slices were rinsed 3 times with PBS and incubated with the secondary antibody (1:400, Abcam, USA) for 30 min. After washing the slices 3 times, DAB solution was applied for color development, followed by rinsing with water and drying. Sections were counterstained with hematoxylin for 3 min, rinsed, dehydrated, sealed, and imaged using a light microscope. The stained slices were then scanned and measured for the optimal density of the stained proteins using Image J software.

#### Western blotting

After extracting total proteins from the ipsilateral hippocampal tissues using RIPA lysis buffer and protease inhibitors (Thermo scientific, USA), the protein concentrations were measured with a BCA assay kit. A total of 30 µg of proteins were separated by a 12% SDS-PAGE gel and transferred to PVDF membranes. The membranes were blocked with 5% skim milk and incubated with the primary antibodies at 4°C overnight. The primary antibodies used in this experiment were as follows: anti-METTL3 (1:10000), anti-METTL14 (1:10000), anti-FTO (1:2000,), anti-Arc (1:10000) and anti-glyceraldehyde 3-phosphate dehydrogenase (GAPDH) (1:20000, Proteintech, USA). After washing, the membranes were incubated with HRP-conjugated anti-mouse or anti-rabbit secondary antibody (1:10000, Proteintech, USA) at RT for 60 min. Finally, these membranes were incubated in ECL Plus reagent for 5 min, and the signals were visualized by exposure to GeneGnome XRQ NPC (SynGene, UK). The results were analyzed using Image J software. The expression levels of these detected proteins were normalized to GAPDH, respectively.

#### Quantitative real-time PCR

Total RNAs from the ipsilateral side of the hippocampal tissues were extracted using TRIzol reagent (Thermo Scientifc, USA) following the manufacturer's protocol. cDNA was synthesized from 1 µg of total RNA using a cDNA Reverse Transcription Kit (TransGen Biotech, China). The gRT-PCR conditions were as follows: 95°C for 10 min and 40 cycles of 95°C for 15 sec, 60°C for 10 min, and 95°C for 15 sec. Melting curve analysis was conducted after the 40th amplification cycle: 95°C for 15 sec, 60°C for 60 sec and 95°C for 15 sec. The qRT-PCR was performed using the PerfectStart ® Green qPCR SuperMix (+Dye II) (TransGen Biotech, China) on the Step One Plus Realtime PCR System (Applied Biosystems, USA). The relative expression of the gene in each sample was obtained by comparison to GAPDH and analyzed using the 2-ΔΔCT method. The primer sequences for qRT-PCR were listed in Table 1.

Table 1. Primer sequences used for qRT-PCR

Gene	Accession number	Primer Sequence (5'→3')	Product size (bp)
METTL3	NM_019721.2	F: TTGCCATCTCTACGCCAGAT	164
		R: CATGGCAGACAGCTTGGAGT	
METTL14	NM_201638.2	F: GGACCTTGGGAGAGTATGCTTG	165
		R: ACGGTTCCTTTGATCCCCAT	
FTO	NM_011936.2	F: GGACATCGAGACACCAGGATT	302
		R: GCCACTCAAACTCCACCTCAT	
Arc	NM_001276684.1	F: GTTGACCGAAGTGTCCAAGCAG	89
		R: CGTAGCCGTCCAAGTTGTTCTC	
GAPDH	NM_001411841.1	F: GGTTGTCTCCTGCGACTTCA	183
		R: TGGTCCAGGGTTTCTTACTCC	

#### Statistical analysis

SPSS software (version 27.0; SPSS, Inc., IL, USA) was used for statistical analyses. All data were presented as the mean±SEM at least three independent experiments. Multiple comparisons between the treated groups and the control were performed using one-way analysis of variance (ANOVA) followed by the post hoc tests (LSD or Tamhane's T2) for the normal distribution or the Mann-Whitney U tests for the skewed distribution. The correlations between the expression levels of Arc and METTL3, as well as fluoride levels in urinary were analyzed by Pearson correlation test. The statistical significance was determined by considering P-values below 0.05.

#### **RESULTS**

# Establishment of the mouse model with chronic fluorosis

After being exposed to fluoride for 3 months, obvious dental fluorosis appeared in the mice (Figure 1A). The enamel transparency of mice in the group fed with 50 ppm NaF decreased, presenting mild turbidity and faintly visible white fine lines (I°). In the group with 100 ppm NaF, the teeth of mice were chalky, the enamel lost its luster, and the overall shape was abnormal (II°). In addition, the fluoride contents in the bones (Figure 1B) and urine (Figure 1C) of mice with fluoride exposure were significantly increased.

Moreover, HE and Nissl staining of brain tissues were used to assess the neuropathological condition of the mice exposed to fluoride. In the hippocampal regions of mice with HE staining of the control group, the regular arrangement of neurons was presented, whereas in the fluoride exposed groups, the loose disordered arrangement of neurons with shrunken and deep staining nuclei were observed (Figure 1D). On the

other hand, the obviously reduced Nissl bodies in neurons were observed in the hippocampus of mice with fluoride exposure compared to controls (Figure 1E).

# Impaired synaptic structure and related proteins in mouse brain exposed to fluoride

In fluoride exposed mice, the neurons in the hippocampus had significantly lower density of dendritic spine (Figure 2A and B) and fewer numbers of dendritic branches (Figure 2C-E) as compared to controls. However, no notable change in dendritic spine or dendritic branch were observed between the 50 ppm and 100 ppm fluoride exposed groups (Figure 2).

The IHC staining results showed that Arc was primarily expressed in the cytosol. The average optical density (AOD) of Arc in the hippocampus of mouse brain exposed to fluoride was significantly reduced as compared with that of the control group (Figure 3A and B). In addition, the decreased expression of Arc protein was also observed by Western blotting in the hippocampal tissues of mice with the exposure of 100 ppm NaF, but no change of Arc at protein level in the group treated with 50 ppm NaF (Figure 3C). For the mRNA level of Arc detected by qRT-PCR, no significant differences occurred in the groups exposed to fluoride as compared to controls (Figure 3D).

## Changed expressions of m6A-related enzymes in in mouse brain exposed to fluoride

IHC staining revealed a significant reduction in the mean AOD of METTL3 protein in the hippocampal region exposed to 50 ppm NaF as compared to the control group, whereas no significant difference was observed in the 100 ppm NaF group (Figure 4A and B). The significant decreases in METTL3 protein expression detected by Western blotting were found in the

hippocampus of mice exposed to fluoride (Figure 4C). No significant changes were detected in METTL3 mRNA level (Figure 4D) or in the protein and mRNA expressions of METTL14 (Figure 5) and FTO (Figure 6) in the fluoride-treated groups as compared to controls.

#### Relationships among Arc, METTL3 and urinary fluoride

We further investigated the association between Arc, METTL3 and urinary fluoride levels of the mice.

Pearson's bivariate correlation and simple linear regression analysis displayed a positive correlation between the reduced levels of Arc protein and the decreased METTL3 protein (Figure 7A). On the other hand, the negative relationships between levels of Arc and urinary fluoride contents (Figure 7B), as well as levels of METTL3 and urinary fluoride contents of the mice with fluorosis were detected (Figure 7C).

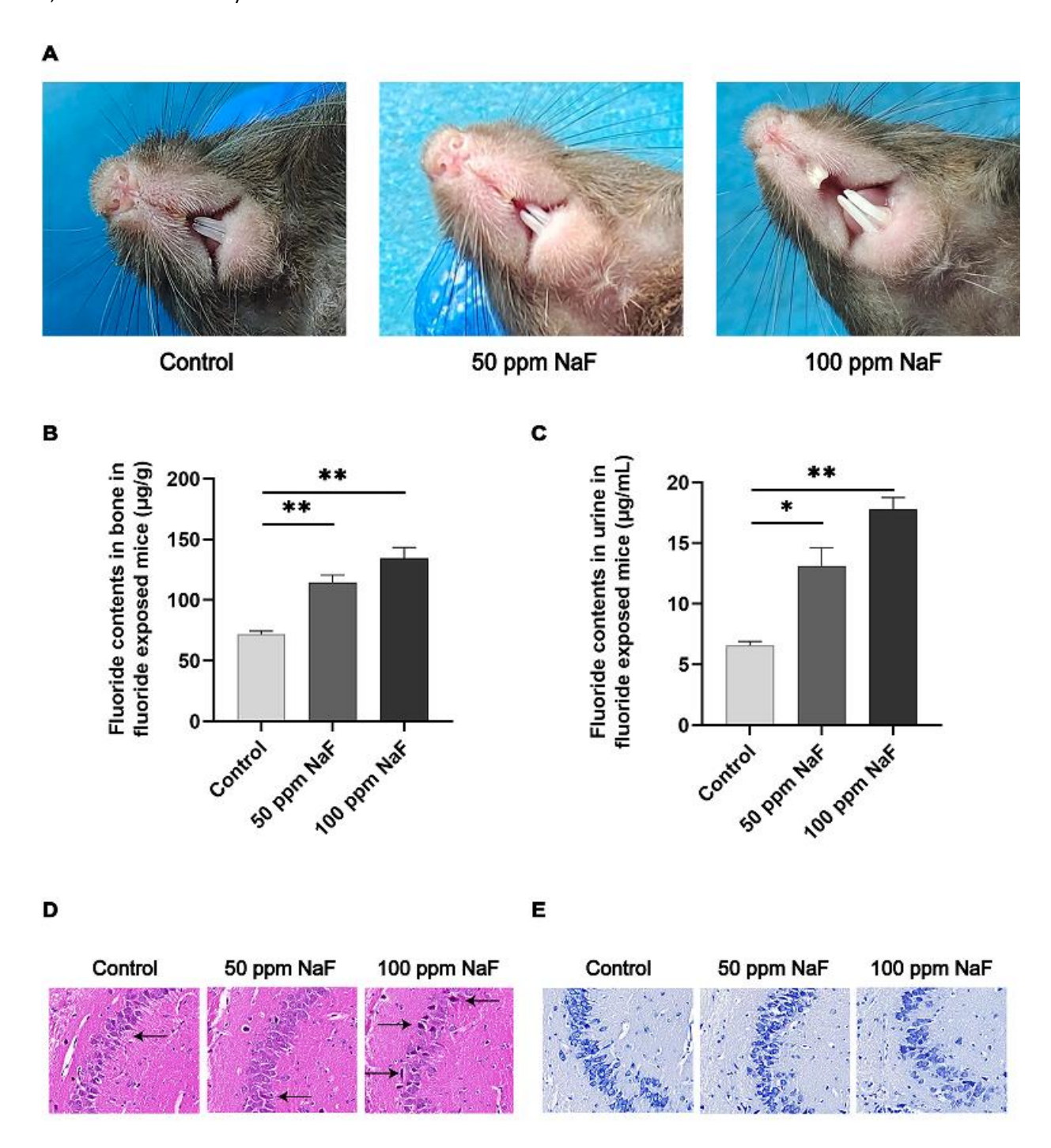


**Figure 1.** Basic conditions and histomorphologic alteration of the hippocampus in mice exposed to different concentrations of fluoride. A: degree of dental fluorosis in the mice. B: fluoride content in bone. C: fluoride content in urine. D: HE staining of the CA3 region of the hippocampus in mice. E: NissI staining of the CA3 region of the hippocampus in mice. The black arrow indicates pyknosis in neurons. Scale bar=50  $\mu$ m, ×400, n=6. \*P< 0.05 or \*\*P< 0.01 compared to the control group

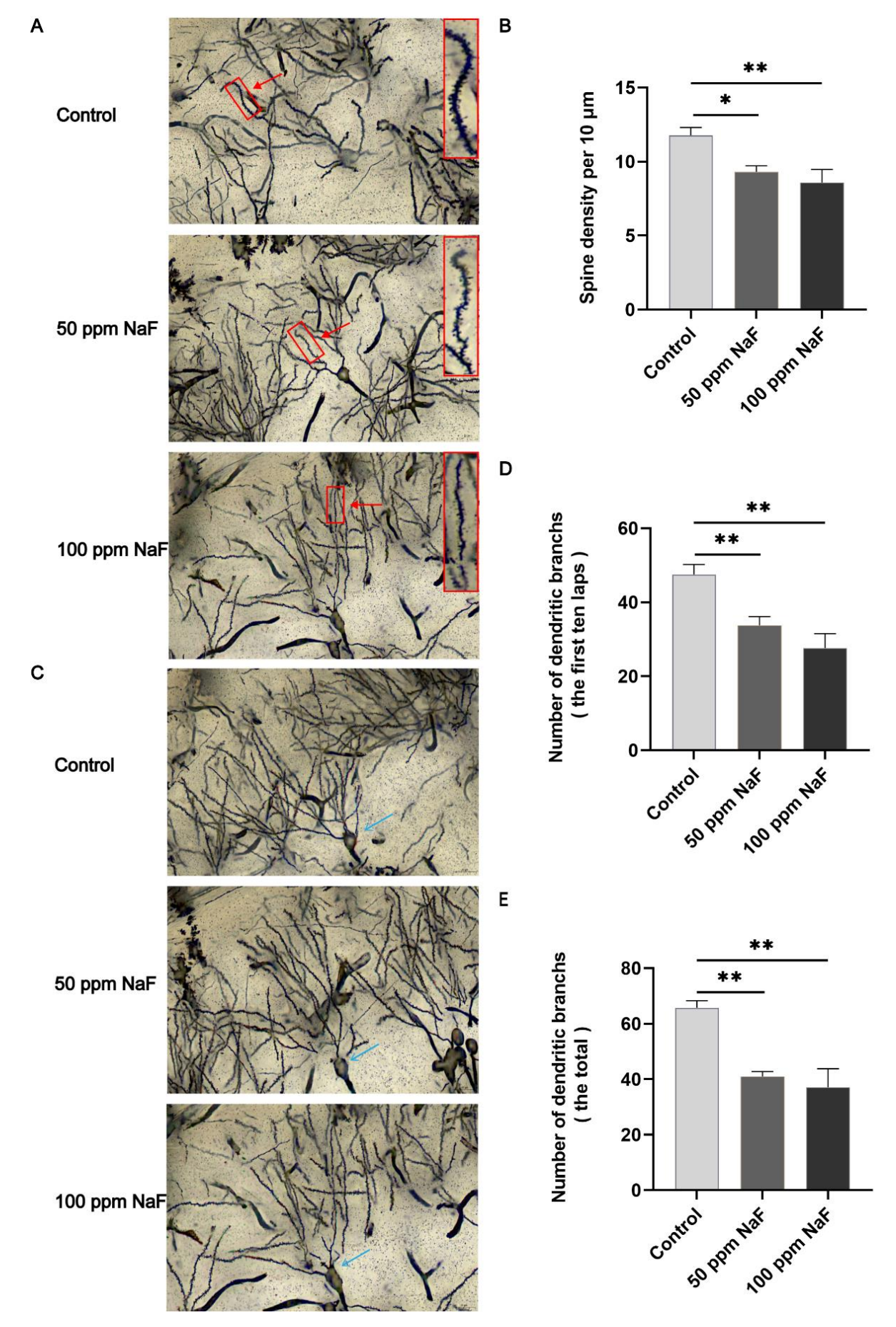
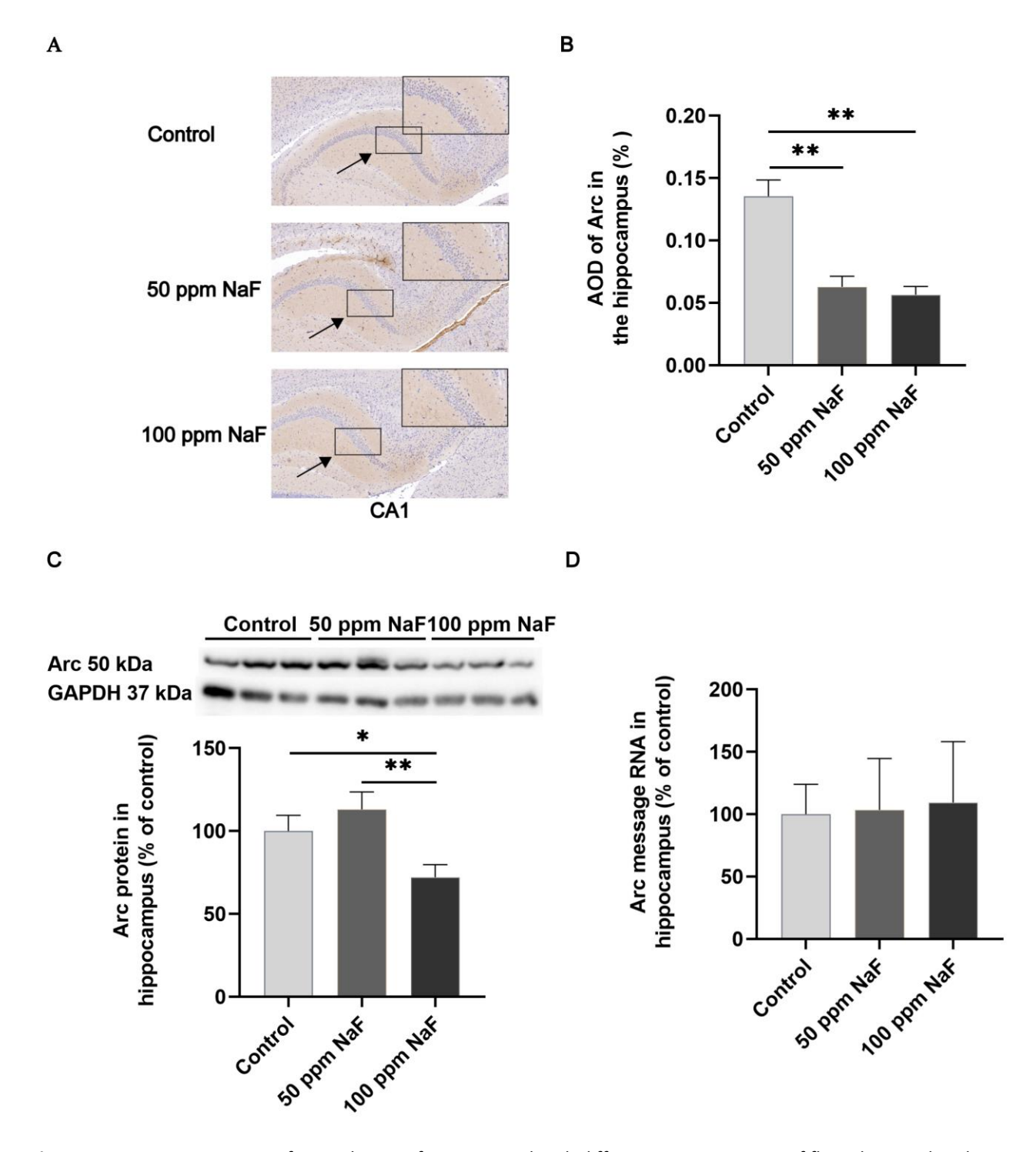


Figure 2. Impaired synaptic structures in mice treated with different concentrations of fluoride. A and B: dendritic spine density in the CA3 region of the hippocampus in mice. C-E: dendritic branches in the CA3 region of the hippocampus in mice. Scale bar =  $20 \mu m$ ,  $\times 600$ , n = 8 neurons from 4 mice. \*P < 0.05 or \*\* P < 0.01 compared to the control group



**Figure 3.** Protein expressions of Arc in brains of mice treated with different concentrations of fluoride. A and B: the IHC staining diagram of Arc in CA1 regions of the hippocampus of mice. C: expression of Arc at proteins level in mice by Western blotting. D: expression of Arc at mRNA level in brain of mice by qRT-PCR. Scale bar =  $50 \mu m$ ,  $\times 400$ , n = 6.\*P < 0.05 or \*\*P < 0.01 compared to the control group

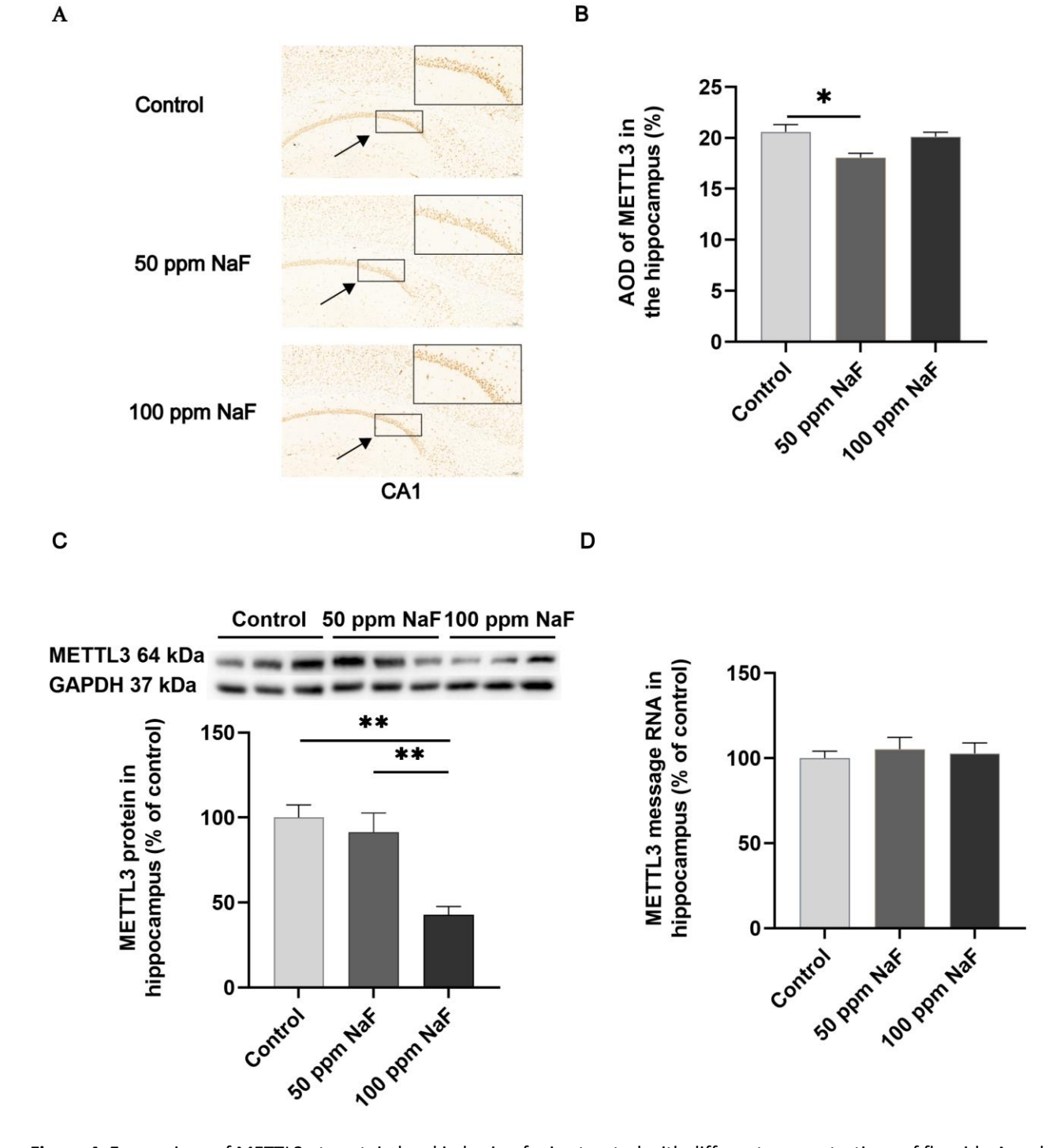
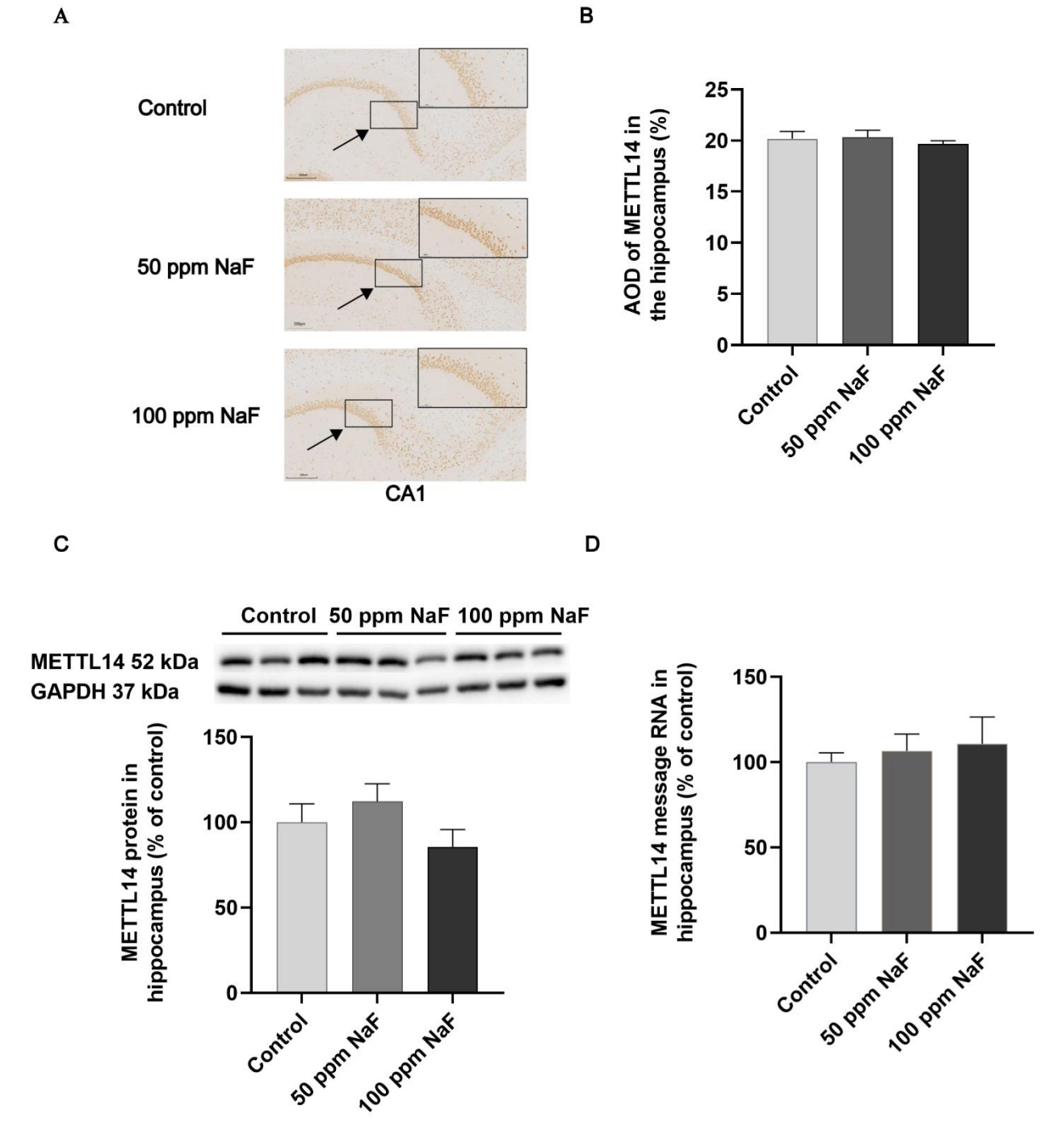
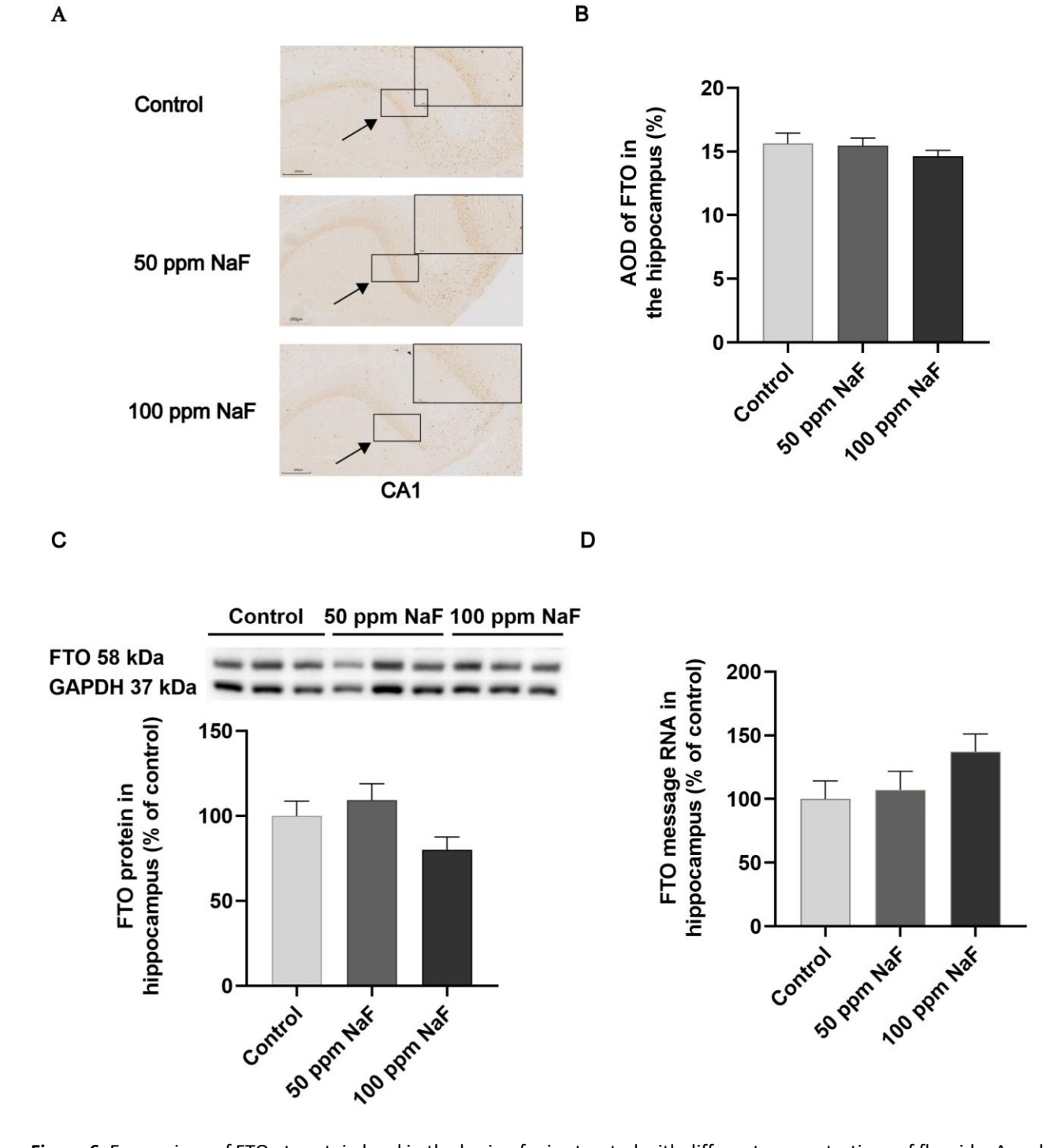


Figure 4. Expressions of METTL3 at protein level in brain of mice treated with different concentrations of fluoride. A and B: the IHC staining diagram of METTL3 in the CA1 regions of the hippocampus in mice. C: expression of METTL3 at protein level in mice detected by Western blotting. D: expression of METTL3 at mRNA level in brain of mice detected by qRT-PCR. Scale bar =  $50 \, \mu m$ , ×400, n = 6. \*P< 0.05 or \*\*P<0.01 compared to the control group



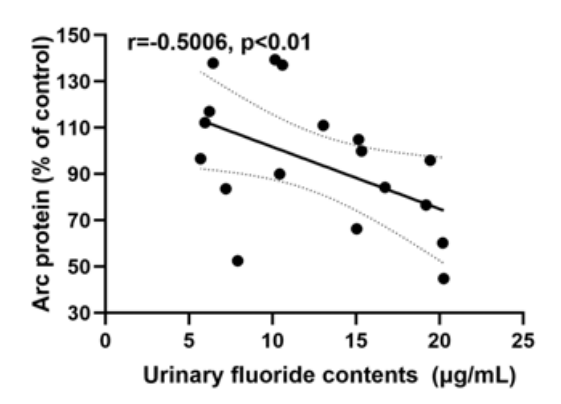
**Figure 5.** Expressions of METTL14 at protein level in brain of mice treated with different concentrations of fluoride. A and B: the IHC staining diagram of METTL14 in the CA1 regions of the hippocampus in mice. C: expression of METTL3 at protein level in mice detected by Western blotting. D: expression of METTL14 at mRNA level in brain of mice detected by qRT-PCR. Scale bar =  $50 \, \mu m$ ,  $\times 400$ , n = 6



**Figure 6.** Expressions of FTO at protein level in the brain of mice treated with different concentrations of fluoride. A and B: the IHC staining diagram of FTO in the CA1 regions of the hippocampus in mice. C: expression of FTO at protein level in mice detected by Western blotting. D: expression of METTL14 at mRNA level in brain of mice detected by qRT-PCR. Scale bar =  $50 \, \mu m$ ,  $\times 400$ , n = 6

Telephone (% of control)

В



С

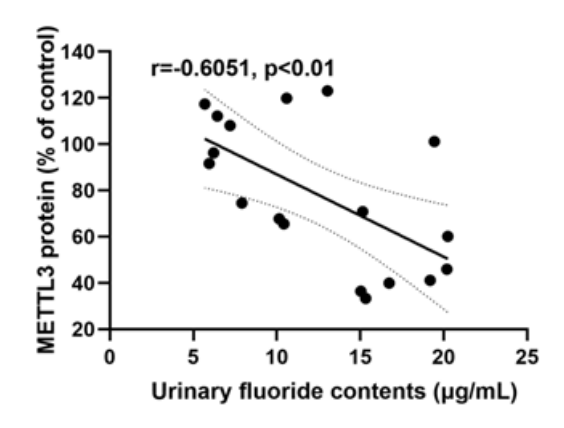


**Figure 7.** Correlations between METTL3 and / or Arc levels in hippocampal tissues of mice and UF contents of mice with chronic fluorosis. (A) Correlations between METTL3 and Arc in hippocampal tissues of mice. (B) Correlations between METTL3 and UF contents. (C) Correlations between Arc and UF contents

#### **DISCUSSION**

In this study, we successfully established a mouse model of chronic fluorosis by adding fluoride to their drinking water for 3 months. The mice developed dental fluorosis and showed the increased level of fluoride in bones and urine, which was consistent with

several previous findings.<sup>19</sup> In addition, in our study here, the histopathological changes in brains of mice with fluorosis were manifested as the disordered arrangement of neurons with shrunken and deep staining nuclei, indicating that the neurons were damaged by fluorosis. Furthermore, the numbers of Nissl bodies in the neurons of the hippocampus of mice with chronic fluorosis were significantly reduced in the study, suggesting that the active state of the neurons was significantly decreased due to fluoride exposure, which is aligned with previous study.<sup>2</sup>

A large number of in vivo and in vitro studies and epidemiological investigations have found that chronic fluorosis can cause brain damage, resulting in abnormal brain structure and function.<sup>20</sup> Interestingly, a decline in hippocampal function has long been associated with the progression of cognitive impairments in patients with neurodegenerative diseases.<sup>21</sup> The patients with cognitive impairment showed the synaptic density of nucleus basalis decreased, exhibiting a worse cognitive performance compared to cognitively normal individuals.<sup>22</sup> Fluoride exposure induced a decrease in the density and co-localization of excitatory synaptic markers, thereby causing impaired development.<sup>23</sup> The lower levels of synaptic proteins and enhanced oxidative stress were also detected in the hippocampus of APP mice aggravated to fluoride.24

Here, we found significantly lower density of dendritic spine and fewer numbers of dendritic branches in the neurons of the hippocampal regions of mice with fluoride exposure. Furthermore, the level of Arc in the hippocampal region of the mouse exposed to fluoride was significantly reduced by both detections with IHC and Western blotting in our study. Extensive research indicates that Arc is crucial for maintaining synaptic structure and affects neuronal plasticity by interacting the neuronal skeleton. 10 Arc-deficient mice showed poor performance in behavioral tasks like the Morris water maze and novel object recognition.<sup>25</sup> Arc knockdown in rats resulted in cognitive deficits in spatial, emotional, and social memory tasks.<sup>26</sup> Whereas, when Arc induction was inhibited, both long-term potentiation and long-term memory were disrupted.<sup>27</sup> However, in this study, we did not find any changes in Arc at the mRNA level, indicating that the modification of Arc by fluoride occurred at the processes after transcription of the molecule.

Neuronal epigenetics is becoming a distinct field in neuroscience, advancing the study of complex systems.<sup>28</sup> In this area, m6A methylation is crucial in neurodevelopment,<sup>29</sup> involving many disorders of brains, such as traumatic brain injury, AD, Parkinson's disease (PD), and other cognitive diseases. As a crucial part of the m6A methyltransferase complex, METTL3 is linked to neurological damage. The expression of METTL3 was notably reduced in the brain and leukocytes of a post-stroke mouse model.<sup>30</sup> In mouse

brain with PD, METTL3 expression was notably reduced and dopamine neuron damaged by activating the METTL3/glutaredoxin axis.<sup>31</sup> Additionally, the effect of METTL3 on neurotoxicity and its impact on the phosphoinositide 3-kinase/protein kinase B pathway downregulation have been recognized.<sup>32</sup>

It was found that fluoride triggered m6A mediated ferroptosis to cause intestinal damage. <sup>14</sup> In the study, we determined the expressions of m6A-associated regulators in the hippocampus of mice exposed to fluoride. A significant reduction of METTL3 was determined in the hippocampus of mice exposed to high dose of NaF, which is similar with published result. <sup>33</sup> qRT-PCR results indicated no significant change of METTL3 at mRNA level, indicating the effect of fluoride on the molecular occurs at the step after transcription. Importantly, since the levels of METTL14 and FTO remained unchanged in our study, we proposed that METTL3 might be a key regulator of m6A modification in hippocampal neurons under exposed situation of fluoride.

METTL3 is mainly found in the nucleus and cytoplasm, while Arc is expressed in the cytoplasm, both of which are closely related. In a study concerning the disturbance of synaptic plasticity, knockdown of METTL3 decreased ARC mRNA m6A modification and reduced Arc protein expression, while overexpression of METTL3 rescued Arc expression influenced by βamyloid peptide (Aβ),<sup>34</sup> suggesting an important mechanism of epigenetic alteration in AD, i.e., Arc may be an m6A-modified target protein of METTL3. In our results, there was a positive correlation between the levels of Arc and METTLs, a negative correlation between the levels of Arc or METTLs and urinary fluoride. We hypothesize that fluoride decreases METTL3 protein expression, which may affect the procedure of Arc mRNA's nuclear export via m6A modification, and ultimately reduce Arc protein level and damage synaptic structure.

#### **CONCLUSION**

In study, the mouse model with chronic fluorosis was established, which presented with dental fluorosis, high contents of fluoride in born and urine, neuropathology of the mice exposed to fluoride. Obviously, the modified synaptic structure of neurons was observed in the brain of such fluorosis mice. Importantly, the protein expression, but mRNAs, of Arc was significantly decreased in mouse brains influenced by fluorosis, which is involved in the changed synaptic structure. Furthermore, the declined METTL3 influenced by fluorosis may be specifically related to the inhibited expression of Arc, because no significant changes of METTL14 and FTO expression were determined in mouse brain exposed to fluoride. Interestingly, the decreased protein level of Arc or

METTL3 in brain was significantly correlated with the increased content of fluoride in urine resulted from fluoride exposure. The results indicated that excessive fluoride intake caused damage to the synaptic structure and reduction of Arc protein in the brain of mice, which in mechanism might be involved to the decreased expression of METTL3.

#### **FUNDING**

This study was financed by grants from the Natural Science Foundation of China (82260668); the Foundation of Guizhou Province of China (ZK [2022]401, ZK [2022]342, ZK[2021]490, GZWKJ2023-225, KY[2021]183, GZWKJ2022-217, GZWKJ2025-530, GZWKJ2025-134, [2019]1276); the Foundation of Guizhou Medical University ([2020]046).

#### **CONFLICT OF INTERESTS**

The authors declare that they have no competing interests.

#### REFERENCES

- [1] Wei N, Guan ZZ. Damage in nervous system. In Guan Z, editor: Coal-burning type of endemic fluorosis – Pathophysiology and Clinical Treatments, Singapore, Springer, 2021, pp 105-124.
- [2] Xiang J, Qi XL, Cao K, Ran LY, Zeng XX, Xiao X, et al. Exposure to fluoride exacerbates the cognitive deficit of diabetic patients living in areas with endemic fluorosis, as well as of rats with type 2 diabetes induced by streptozotocin via a mechanism that may involve excessive activation of the poly(ADP ribose) polymerase-1/P53 pathway. Sci Total Environ 2024;912:169512. doi.org/10.1016/j.scitotenv.2023.169512.
- [3] Saeed M, Malik RN, Kamal A. Fluorosis and cognitive development among children (6-14 years of age) in the endemic areas of the world: a review and critical analysis. Environ Sci Pollut Res Int 2020;27:2566-2579. doi.org/10.1007/s11356-019-06938-6
- [4] Nagarajappa R, Pujara P, Sharda AJ, Asawa K, Tak M, Aapaliya P, et al. Comparative assessment of intelligence quotient among children living in high and low fluoride areas of kutch, India-a pilot study. Iran J Public Health 2013;42:813-818.
- [5] Agalakova NI, Nadei OV. Inorganic fluoride and functions of brain. Crit Rev Toxicol 2020;50:28-46. doi.org/10.1080/10408444.2020.1722061
- [6] Lai C, Chen Q, Ding Y, Liu H, Tang Z. Emodin protected against synaptic impairment and oxidative stress induced by fluoride in SH-SY5Y cells by modulating ERK1/2/Nrf2/HO-1 pathway. Environ Toxicol 2020;35:922-929. doi.org/10.1002/tox.22928
- [7] Qian W, Miao K, Li T, Zhang Z. Effect of selenium on fluorideinduced changes in synaptic plasticity in rat hippocampus. Biol Trace Elem Res 2013;155:253-260. doi.org/10.1007/s12011-013-9773-x
- [8] Zhang J, Xu P, Zhang Y, Li T, Ding X, Liu L, et al. Unraveling the role of abnormal AMPK and CRMP-2 phosphorylation in

- developmental fluoride neurotoxicity: Implications for synaptic damage and neurological disorders. Ecotoxicol Environ Saf 2025;296:118192. doi: 10.1016/j.ecoenv.2025.118192
- [9] Wilkerson JR, Albanesi JP, Huber KM. Roles for Arc in metabotropic glutamate receptor-dependent LTD and synapse elimination: Implications in health and disease. Semin Cell Dev Biol 2018;77:51-62. doi.org/10.1016/j.semcdb.2017.09.035
- [10] Chen Y, Wang X, Xiao B, Luo Z, Long H. Mechanisms and functions of activity-regulated cytoskeleton-associated protein in synaptic plasticity. Mol Neurobiol 2023;60:5738-5754. doi.org/10.1007/s12035-023-03442-4
- [11] Yang N, Higuchi O, Ohashi K, Nagata K, Wada A, Kangawa K, et al. Cofilin phosphorylation by LIM-kinase 1 and its role in Rac-mediated actin reorganization. Nature 1998;393:809-812. doi.org/10.1038/31735
- [12] Xia W, Liu Y, Lu J, Cheung HH, Meng Q, Huang B. RNA methylation in neurodevelopment and related diseases. Acta Biochim Biophys Sin (Shanghai) 2024;56:1723-1732. doi.org/10.3724/abbs.2024159
- [13] Meyer KD, Saletore Y, Zumbo P, Elemento O, Mason CE, Jaffrey SR. Comprehensive analysis of mRNA methylation reveals enrichment in 3' UTRs and near stop codons. Cell 2012;149:1635-1646. doi.org/10.1016/j.cell.2012.05.003
- [14] Huang H, Lin Y, Xin J, Sun N, Zhao Z, Wang H, et al. Fluoride exposure-induced gut microbiota alteration mediates colonic ferroptosis through N6-methyladenosine (m6A) mediated silencing of SLC7A11. Ecotoxicol Environ Saf 2024;283:116816. doi: 10.1016/j.ecoenv.2024.116816.
- [15] Merkurjev D, Hong WT, lida K, Oomoto I, Goldie BJ, Yamaguti H, et al. Synaptic N(6)-methyladenosine (m(6)A) epitranscriptome reveals functional partitioning of localized transcripts. Nat Neurosci 2018;21:1004-1014. doi.org/10.1038/s41593-018-0173-6
- [16] Koranda JL, Dore L, Shi H, Patel MJ, Vaasjo LO, Rao MN, et al. Mettl14 is essential for epitranscriptomic regulation of striatal function and learning. Neuron 2018;99:283-292.e285. doi.org/10.1016/j.neuron.2018.06.007
- [17] Han M, Liu Z, Xu Y, Liu X, Wang D, Li F et al. Abnormality of m6A mRNA methylation is involved in Alzheimer's Disease. Front Neurosci 2020;14:98. doi.org/10.3389/fnins.2020.00098
- [18] Dean, H. T. Endemic fluorosis and its relation to dental caries. 1938. Nutrition 1990;6:435-445.
- [19] Ran LY, Xiang J, Zeng XX, He WW, Dong YT, Yu WF, et al. The influence of NQO2 on the dysfunctional autophagy and oxidative stress induced in the hippocampus of rats and in SH-SY5Y cells by fluoride. CNS Neurosci Ther 2023;29:1129-1141. doi.org/10.1111/cns.14090
- [20] Ren C, Li HH, Zhang CY, Song XC. Effects of chronic fluorosis on the brain. Ecotoxicol Environ Saf 2022;244:114021. doi.org/10.1016/j.ecoenv.2022.114021.
- [21] Good MA, Bannerman DM. Hippocampal synaptic plasticity: integrating memory and anxiety impairments in the early stages of Alzheimer's Disease. Curr Top Behav Neurosci 2025;69:27-48. doi.org/10.1007/7854\_2024\_565.
- [22] Li B, Chen H, Zheng Y, Xu X, You Z, Huang Q, et al. Loss of synaptic density in nucleus basalis of meynert indicates distinct neurodegeneration in Alzheimer's disease: the RJNB-D study. Eur J Nucl Med Mol Imaging 2024;52(1):134-144. doi.org/10.1007/s00259-024-06862-z.
- [23] Qiu W, Wang X, Zhang S, Zhang Z, Zhang K, Shao Z, et al. Dose-dependent developmental fluoride exposure leads to

- neurotoxicity and impairs excitatory synapse development. Arch Toxicol 2025 Mar 14; doi.org/10.1007/s00204-025-04003-5.
- [24] Cao K, Xiang J, Dong YT, Xu Y, Li Y, Song H, et al. Exposure to fluoride aggravates the impairment in learning and memory and neuropathological lesions in mice carrying the APP/PS1 double-transgenic mutation. Alzheimers Res Ther 2019;11(1):35. doi.org/10.1186/s13195-019-0490-3.
- [25] Kedrov AV, Durymanov M, Anokhin KV. The Arc gene: Retroviral heritage in cognitive functions. Neurosci Biobehav Rev 2019;99:275-281. doi.org/10.1016/j.neubiorev.2019.02.006.
- [26] Okuno H, Minatohara K, Bito H. Inverse synaptic tagging: An inactive synapse-specific mechanism to capture activityinduced Arc/arg3.1 and to locally regulate spatial distribution of synaptic weights. Semin Cell Dev Biol 2018;77:43-50. doi.org/10.1016/j.semcdb.2017.09.025.
- [27] Steward O, Worley P. Local synthesis of proteins at synaptic sites on dendrites: role in synaptic plasticity and memory consolidation? Neurobiol Learn Mem 2002;78:508-527. doi.org/10.1006/nlme.2002.4102
- [28] Campbell RR, Wood MA. How the epigenome integrates information and reshapes the synapse. Nat Rev Neurosci 2019;20:133-147. doi.org/10.1038/s41583-019-0121-9
- [29] Weng YL, Wang X, An R, Cassin J, Vissers C, Liu Y, et al. Epitranscriptomic m(6)A regulation of axon regeneration in the adult mammalian nervous system. Neuron 2018;97:313-325.e316. doi.org/10.1016/j.neuron.2017.12.036
- [30] Fan J, Zhong L, Yan F, Li X, Li L, Zhao H, et al. Alteration of N6-methyladenosine modification profiles in the neutrophilic RNAs following ischemic stroke. Neuroscience 2024;553:56-73. doi.org/10.1016/j.neuroscience.2024.06.014
- [31] Gong X, Huang M, Chen L. NRF1 mitigates motor dysfunction and dopamine neuron degeneration in mice with Parkinson's disease by promoting GLRX m(6) A methylation through upregulation of METTL3 transcription. CNS Neurosci Ther 2024;30:e14441. doi.org/10.1111/cns.14441
- [32] Ai S, Li D, Gu X, Xu Y, Wang Y, Wang HL, et al. Profile of N6-methyladenosine of Pb-exposed neurons presents epitranscriptomic alterations in PI3K-AKT pathway-associated genes. Food Chem Toxicol 2023;178:113821. doi.org/10.1016/j.fct.2023.113821
- [33] Yang L, Chen L, Li W, Zhang Y, Yang G, Huang B, et al. METTL3-mediated m6A RNA methylation was involved in aluminum-induced neurotoxicity. Ecotoxicol Environ Saf 2024;270:115878. doi.org/10.1016/j.ecoenv.2023.115878
- [34] Xu C, Huang H, Zhang M, Zhang P, Li Z, Liu X, et al. Methyltransferase-Like 3 rescues the amyloid-beta proteininduced reduction of activity-regulated cytoskeleton associated protein expression via YTHDF1-dependent N6methyladenosine modification. Front Aging Neurosci 2022;14:890134. doi.org/10.3389/fnagi.2022.890134.